# Chapter 13
# Methodologies for Mapping Land Cover/Land Use and its Change

**Nina Siu-Ngan Lam**

## 13.1 Introduction

Mapping and identifying land cover/land use and its change is the most important, as well as the most widely researched, topic in remote sensing. Land cover/land use has been used extensively to derive a number of biophysical variables, such as vegetation index, biomass, and carbon content (see other chapters). More importantly, land cover/land use pattern and its change reflect the underlying natural and/or social processes, thus providing essential information for modeling and understanding many different phenomena on the Earth. Knowledge of land cover/land use and its change is also critical to effective planning and management of natural resources.

Mapping land cover/land use accurately and efficiently via remote sensing requires good image classification methods. Unfortunately, there are numerous factors (e.g., image resolution and atmospheric condition) that could affect the effectiveness and accuracy of the classification algorithms. Different land cover/land use classification methods may be needed for different problems under different environmental conditions, making generalization and hence automation of the image classification process across time and space extremely difficult. As a result, new and sophisticated classification methods designed to improve the classification process continue to appear in the literature (e.g., Jensen, 2005; Gong, 2006). Newer approaches such as fuzzy classification, artificial neural network, and object-based classification have been developed and successfully applied (Definiens, 2004; Benz et al., 2004). However, these methods require extensive training and human supervision. We are still far from being able to develop a common framework to successfully identify a variety of features in different landscapes and to generalize and automate the classification process.

Nina Siu-Ngan Lam
Department of Environmental Studies, Louisiana State University, Baton Rouge, USA
nlam@lsu.edu

S. Liang (ed.), *Advances in Land Remote Sensing*, 341–367.

Extending the mapping and modeling of land cover/land use at one time period to multiple time periods to analyze change will undoubtly add more complexity and challenges. In addition to the above image classification issues, efficient methods are needed to ensure comparability and compatibility of images taken in different time periods. Many studies on change detection using remote sensing imagery have already been reported in the literature. Lunetta and Elvidge (1998) provided an excellent summary of the state of the science. Many others examined the performance of various techniques in various applications (e.g., Coppin and Bauer, 1996; Jensen et al., 1993, 1997; Lu et al., 2005; Mas, 1999; Nackaerts et al., 2005; Yuan et al., 1998).

Among the new techniques for land cover/land use classification and change analysis, textural (spatial) analyses are gaining increasing attention from the remote sensing community (e.g., Briggs and Nellis, 1991; Dunn et al., 1991; Estreguil and Lambin, 1996; Frank, 1984; Jupp et al., 1986; Lambin, 1996; Lambin and Strahler, 1994; Pickup and Foran, 1987; Smits and Annoni, 2000; Crews-Meyer, 2002). We have seen new applications of old textural measures such as the spatial co-occurrence matrix, local variance, and others (Haralick et al., 1973; Clausi and Jobanputra, 2006), as well as development of new textural analytical techniques such as wavelets (Daubechies, 1990; Muneeswaran et al., 2005). A number of textural measures which had not been used for remote sensing applications before have recently been utilized for more accurate land cover/land use classification, such as fractals, variograms, lacunarity, and spatial autocorrelation statistics (Lam, 1990; Lam and De Cola, 1993; Plotnick et al., 1993; Lam et al., 1998; Carr and de Miranda, 1998; Carr, 1999; Dale, 2000; Dong, 2000; Franklin et al., 2000). Although applications of these newer textural measures in change analysis have seldom been reported, we expect that the same textural and spatial methods that can be used for identification of land cover/land use can also be used for change detection.

The purpose of this chapter is to introduce the use of textural/spatial measures in land cover/land use classification and its potential for change analysis. Our main notion is that the utilization of textural/spatial measures, in combination with original spectral information, will increase classification accuracy and have great potential for rapid change detection. The chapter is organized into four main sections. A summary of the major textural/spatial methods is first provided in Section 13.2, with a focus on those measures that can be applied directly to unclassified images. This property is important for rapid image segmentation, classification, and change detection. Section 13.3 describes a number of examples that have utilized these measures in land cover/land use classification. In Section 13.4, a framework for classifying the various land cover/land use change detection methods is introduced. We argue for the need to develop innovative methods for rapid and reliable change detection especially during disastrous and unexpected events. We further argue that such need could be best served by utilizing a metric of textural/spatial measures, in conjunction with the original spectral information of the images. Section 13.5 describes a real example of change analysis using textural measures. The prospect of utilizing textural measures in combination with other approaches for better and faster mapping of land cover/land use and its change is summarized in the conclusion.

## 13.2 Major Textural/Spatial Measures

### *13.2.1 Terminology*

First, some clarification of the terms textural vs spatial measure is in order. The term "textural" is more commonly used in pattern recognition and the general field of image processing for raster/pixel data, while the term "spatial" is usually adopted in geography, economics, statistics and other related disciplines and is derived mostly for vector/polygonal data.

Texture is an important characteristic in many types of images. Despite its importance, a formal definition of texture does not exist. Haralick (1979) attempted to characterize texture using two properties, the tonal primitive properties as well as the spatial interrelationships among them. Under this two-layered tone-texture concept, when an image has little variation of tonal primitives, the dominant property of that image is tone. On the contrary, when an image has wide variation of tonal primitives, the dominant property of that image is texture. Haralick described eight statistical approaches to measure image texture, which include autocorrelation functions, optical transforms, digital transforms, textural edgeness, structural elements, spatial gray tone co-occurrence probabilities, gray tone run lengths, and autoregressive models.

In remote sensing, texture is the spatial relationship exhibited by gray levels in a digital image. Therefore, textural measures are measures that capture the spatial relationship among pixels. Spatial measures, which refer to measures mostly derived from spatial statistics, have been used largely in geospatial applications for characterizing and quantifying spatial patterns and processes Although traditionally the two fields of studies, textural analysis and spatial analysis, refer to quite different sets of methods and analyses, they do intersect to a great extent in remote sensing. In this chapter, we adopt the notion that the two terms, textural and spatial measures, are interchangeable.

### *13.2.2 Criteria for Evaluating and Classifying Textural Measures*

There are numerous textural measures in the literature, and it is beyond the scope of this chapter to exhaust and evaluate each of them. Table 13.1 lists some of the commonly used measures, which illustrates clearly the diversity, as well as redundancy, of these various measures. It is important to note that some measures are based on vigorous statistical theory and mathematical derivation (e.g., fractals, wavelets, spatial autocorrelation) (Lam et al., 1998), while others are based on simple geometric measurements with unknown statistical properties and/or theoretical minimum or maximum (e.g., edge density). Some metrics measure one aspect of the landscape (e.g., landscape composition), while others measure another (e.g., landscape configuration) (McGarigal and Mark, 1995). Baskent and Jordan (1995) classified

**Table 13.1** Some commonly used textural measures

| Textural measures | References |
|---|---|
| First-order metrics (computed on the original data matrix) using traditional statistical measures: mean, standard deviation, variance, correlation | Jensen (2005); Gong et al. (1992); Woodcock and Strahler (1987) |
| First-order metrics using traditional texture measures: entropy, energy, contrast, homogeneity, angular second moment, Shannon diversity | Haralick (1979); Haralick et al. (1973); Jensen (2005); Gong et al. (1992) |
| First-order metrics using adapted spatial measures (from ICAMS): fractal dimension, lacunarity, spatial autocorrelation, variogram | Lam et al. (1998, 2002); Quattrochi et al. (1997); Myint and Lam (2005a, b) |
| Second-order metrics: same set of metrics calculated on matrix derived from the original matrix (e.g., gray-level co-occurrence matrix, wavelet decomposed images) | Haralick (1979); Haralick et al. (1973); Myint et al. (2002, 2004) |
| Landscape indices designed for classified images (from FRAGSTATS): area, density, edge, shape, proximity, connectivity, contagion/interspersion, diversity | McGarigal and Mark (1995); McGarigal (2002) |

landscape indices into areal, linear, and topological. Yet another classification of textural measures is based on whether the measures are applied directly to the original matrix (first-order textural measures), or to matrices derived from the original matrix such as the gray-level co-occurrence matrix or wavelet decomposed images (second-order textural measures) (Jensen, 2005). Hence, it is imperative to develop useful criteria to evaluate and/or classify these textural measures. What is a good textural measure? Although there may be no definite answers until each measure is tested extensively for their discriminating and explanatory power, we suggest the following criteria to evaluate and guide our understanding of these various measures.

Ideally, a good textural measure should have the following properties:

1. *The textural measure should be conceptually simple and easy to calculate*. For example, statistical mean and standard deviation are concepts easily grasped by most researchers and their statistical properties are well known. Extension of these basic statistical measures in a spatial domain with some modifications may provide a useful first approximation towards an understanding of the land cover/land use pattern being studied. On the contrary, some measures may be conceptually simple but require additional steps for calculation, such as edge density, which needs an additional step to find the edges.
2. *The textural measure should have theoretical maximum and minimum*. For example, Moran's $I$, a most commonly used spatial autocorrelation statistic, has a range of $\pm 1$. A Moran's $I$ value of 1 indicates a maximum positive spatial autocorrelation; on the contrary, a $-1$ indicates a maximum negative spatial autocorrelation (Cliff and Ord, 1973).
3. *The textural measure should reflect clearly and intuitively the characteristics of the image pattern in a consistent manner*. For example, a lower fractal dimension value means a less spatially complex image, therefore, given an image

computed with a fractal dimension value of 2.3, we should be able to infer that this image is far less complex than an image computed with a fractal dimension value of 2.9, and a visual display of the two images should be able to reveal the difference (Lam, 1990). Fractal dimension $(D)$ also has the second property, where $D$ is expected to range from 2 to 3.0 for surfaces and 1.0–2.0 for lines (Mandelbrot, 1982).

4. *The statistical properties of the textural measure should be known to provide statistical confidence of the computed value*. For example, theoretically a Moran's $I$ value of 0 indicates a random pattern. If a pattern yields a computed value of 0.2, can we determine if this value is statistically the same or different from 0 to conclude if the pattern is random or not? Fortunately, the statistical properties of Moran's $I$ are relatively well known and hypothesis testing of whether a computed $I$ value is significant can be conducted. Under the assumption of randomization, the first and second moments of the Moran's $I$ value can be computed and the statistical significance of the value determined (Goodchild, 1986). On the contrary, the statistical properties of fractal dimension are still not clear, though it has well-defined theoretical minimum and maximum. Hence, it is difficult to judge, for example, if an image with a fractal dimension of 2.3 is significantly different from another image with a fractal dimension of 2.4. It is noted that the statistical properties of most spatial measures are very difficult to derive and therefore remain unclear; many researchers have resorted to the Monte Carlo approach to develop empirical probability functions for statistical hypothesis testing (e.g., Openshaw, 1989).
5. *The textural measure should be computable globally for the entire study area or locally for a local neighborhood*. For example, some landscape metrics developed in FRAGSTATS are only computable at the landscape level, instead of at all levels (patch, class, and landscape) (McGarigal, 2002), whereas mean, variance, Moran's $I$, and fractals can be applied both globally and locally to capture local change (Lam, 2004; Emerson et al., 2005). This property refers only to whether the measure can be computed at all levels; it does not necessarily imply that the measure is useful in describing the landscape at all levels.
6. Finally, *the textural measure should be applicable directly to both classified and unclassified images*. For example, the landscape metrics in FRAGSTATS were developed exclusively for categorical maps (O'Neill et al., 1998; McGarigal, 2002), or in other words, classified images, though some of the metrics can be modified and applied to unclassified images. On the contrary, fractals, Moran's $I$, local variance (Woodcock and Strahler, 1987), variogram, lacunarity, and wavelet measures can be applied to both unclassified and classified images.

This last property is considered very important to automated land cover/land use classification and change detection for two reasons. First, if they can be applied directly to unclassified images, land cove change could be detected first before the tedious classification process. Only after the change is determined to be significant, then there is a need to identify or classify what the changes are. This is considered a more efficient approach, especially for continuous environmental monitoring. Second, since these textural methods measure the spatial variations among

pixels instead of comparing pixel by pixel, they are more likely to reflect dominant changes rather than spurious changes that might have resulted from using images taken in different time periods (Lambin, 1996; Smits and Annoni, 2000). If there are only small and insignificant changes in land cover, it is expected that the spatial relationship will not alter and the spatial index values will remain the same. On the contrary, if there are significant land-cover changes, then it is expected that the spatial properties will be altered, and the spatial indices that are designed to measure the spatial properties should be able to capture these changes.

### *13.2.3 Description of Selected Textural Measures*

We describe below four textural measures, including spatial autocorrelation (Moran's *I*), fractal, lacunarity, and wavelet transform. All four methods have already been implemented in a software module called ICAMS (Image Characterization And Modeling System), developed previously by the author and collaborators (Quattrochi et al., 1997; Lam et al., 1998, 2002; Emerson et al., 1999). ICAMS was developed mainly to provide spatial analytical tools, such as fractals, variograms, and spatial autocorrelation, to visualize, measure, and characterize landscape patterns. Detailed descriptions of ICAMS can be found in a number of publications (e.g., Quattrochi et al., 1997; Lam et al., 1997, 1998). The four methods were selected for illustration because they at least have properties 5 and 6 (can apply locally and to unclassified images), which are important properties for rapid classification and change detection. Furthermore, Moran's *I* possesses all properties, fractals have all but property 4. Lacunarity is an old measure but its use in land cover/land use analysis is relatively new, its properties remain to be thoroughly studied (Myint and Lam, 2005a, b). The mathematics of wavelet transformation is well defined. However, the properties of the textural measures computed on the wavelet transformed images have seldom been studied, and will be a subject of our ongoing research.

#### 13.2.3.1 Spatial Autocorrelation

Spatial autocorrelation statistic has been commonly used to measure the degree of clustering, randomness, or fragmentation of a spatial pattern. The two most common spatial autocorrelation measures for interval-ratio data are Moran's *I* and Geary's *C* (Cliff and Ord, 1973). Moran's *I* is generally preferred over Geary's *C*, because the values of the former are more intuitive (i.e., positive values for positive autocorrelation and vice versa). Moran's *I* was also found to be generally more robust (Goodchild, 1986). These two measures were originally developed for measuring polygonal data (e.g., geographical regions) where the number of units or points measured $(n)$ is often smaller. It is only recently that these two measures were applied to raster data such as remotely sensed images, where the number of units being

measured $(n \times n)$ is much larger (Emerson et al., 1999; Lam et al., 2002). Moran's $I$ is calculated from the following formula:

$$I(d) = \frac{\sum_i^n \sum_j^n w_{ij} z_i z_j}{w \sum_i^n z_i^2} \tag{13.1}$$

where $w_{ij}$ is the weight at distance $d$ so that $w_{ij} = 1$ if point $j$ is within distance $d$ from point $i$; otherwise, $w_{ij} = 0$; $z$'s are deviations from the mean for variable $y$, and $w$ is the sum of all the weights where $i \neq j$. Moran's $I$ varies from $+1$ for perfect positive correlation (a clumped pattern) to $-1$ for perfect negative correlation (a checkerboard pattern). Figure 13.1 shows three simulated surfaces and their corresponding Moran's $I$ and fractal dimension values. Moran's $I$ and fractal

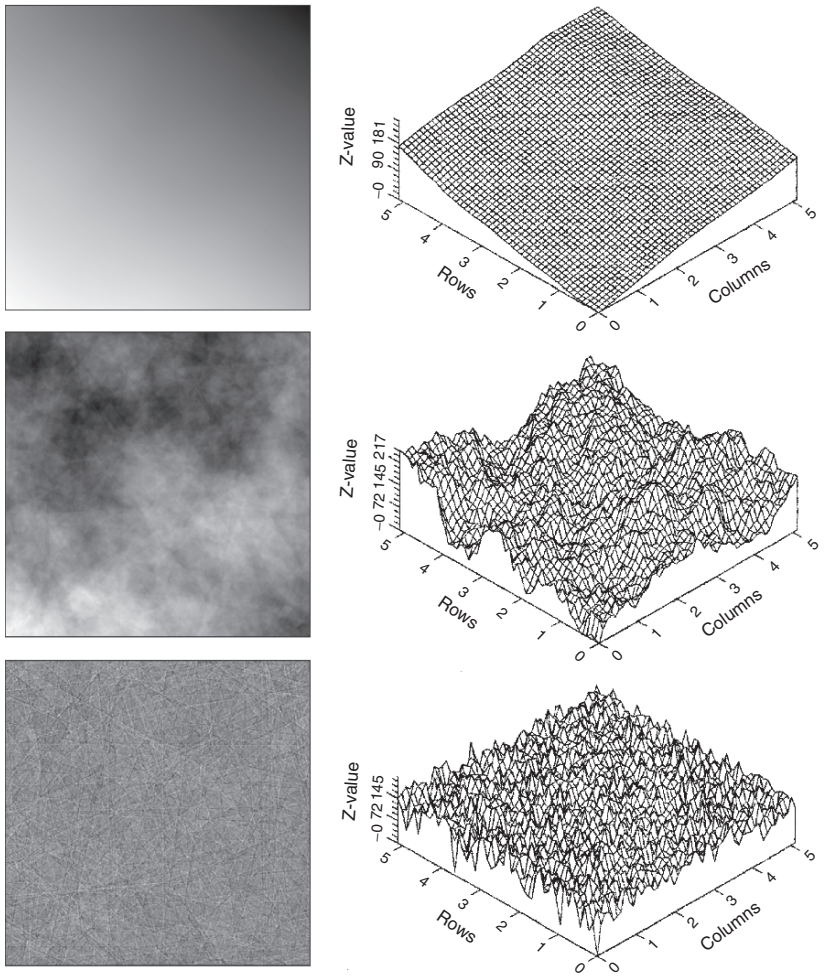


**Fig. 13.1** Three simulated surfaces mapped in three-dimensional and image forms. From top to bottom, $D = 2.1$, 2.5, 2.9, and $I = 1.0$, 0.99, 0.82. (Modified from Lam et al., 2002.)

dimension ($D$) have an inverse relationship, whereby a spatial pattern with a high degree of fragmentation will have a low Moran's $I$ but a high fractal dimension.

#### 13.2.3.2 Fractal Dimension

Fractals were derived mainly to overcome the difficulty in analyzing spatial forms and processes by classical Euclidean geometry. The key parameter in fractals is fractal dimension $D$, which is used to represent the complexity of spatial forms and processes. The higher the $D$, the more complex is the curve or surface. The $D$ value of a curve can be any non-integer value between 1 and 2, and a surface between 2 and 3. For example, coastlines have dimension values typically around 1.2, and topographic surface dimensions around 2.3. Dimension values for satellite image surfaces have been reported to be much higher, and depending on the type of landscapes examined, they can be as high as 2.7–2.9 (Lam, 1990; Jaggi et al., 1993).

Fractal dimension is derived from the concept of self-similarity, where a curve or a surface is made up of copies of itself in a reduced scale (Mandelbrot, 1982). The number of copies ($m$) and the scale reduction factor ($r$) can be used to determine the dimensionality of the curve or surface, where $D = -\log(m)/\log(r)$ (Falconer, 1988). Practically the $D$ value of a curve is estimated by measuring the length of the curve using various step sizes. The more irregular the curve, the greater increase in length as step size decreases. Such an inverse relationship between total line length and step size can be captured by a regression:

$$log(L) = C + B\, log(G) \tag{13.2}$$

where $L$ is the line length, $G$ is the step size, $B$ is the slope of the regression, and $C$ is a constant. $D$ can be calculated by: $D = 1 - B$. For surfaces, $D = 2 - B$.

Because of its attractive theoretical foundation, literally every major discipline has found applications using the fractal concept in the past two decades, with numerous algorithms developed for computing the fractal dimension. Unfortunately, a major problem in applying fractals is that different fractal measurement algorithms yield different results. Often times, empirically computed fractal dimensions may exceed the theoretical ranges. Moreover, fractal dimension is defined in various ways in different algorithms. For example, some algorithms use only a single measurement to derive the dimension, instead of using multiple step sizes to derive the dimension through regression analysis. FRAGSTATS defines fractal dimension as the ratio between perimeter and area of a patch, which is very different from the algorithms described below (Lam, 1990). The former definition of fractal dimension, though simple and easy to calculate, applies only to images that have already been classified, whereas the algorithms described below (e.g., the triangular prism algorithm) follow closely the original definition by Mandelbrot and can be applied directly to unclassified images for textural comparison.

Lam (1990) demonstrated the use of three methods, including isarithm, triangular prism, and variogram methods, in measuring the spatial complexity of the reflectance surfaces from remote sensing imagery (Goodchild, 1980; Clarke, 1986;

Mark and Aronson, 1984). In a subsequent benchmark study, Lam et al. (2002) found that the modified triangular prism method was the most accurate and reliable method for estimating the fractal dimension of surfaces. Hence, the modified triangular prism method is described as follows.

The modified triangular prism method (Clarke, 1986; Jaggi et al., 1993; Lam et al., 2002) constructs triangles by connecting the heights or $z$-values at the four corners of a grid cell to its center, with the center height being the average of the pixels at the four corners. These triangular "facets" of the prism are then summed to represent the surface area. In the second step, the algorithm increases the step size from one pixel to two pixels, and the $z$-values at the four corners of the $2 \times 2$ composites are used to construct the prism. It is expected that as step size increases, the prism surface area will increase, but at a decreasing rate, which can then be used to determine the fractal dimension by a regression equation similar to Eq. (13.2): $Log\ A = K + (2 - D)\ Log\ S$, where $A$ is the prism surface area, $K$ is a constant, $D$ is the fractal dimension, and $S$ is the pixel size.

#### 13.2.3.3 Lacunarity

Despite the potential of fractals, Mandelbrot (1982) realized that fractal dimensions are very far from providing a complete characterization of spatial forms. He introduced the term lacunarity (lacunar in Latin means gap) to further describe the gappiness or texture of a spatial pattern. In other words, different fractal sets may have the same fractal dimension values, but they may look different because they have different lacunarities (Myint and Lam, 2005a).

Lacunarity represents the distribution of gap sizes; low lacunarity implies homogeneity as all gap sizes are the same, whereas high lacunarity implies heterogeneity (Dong, 2000). Unfortunately, lacunarity is highly sensitive to scale, and depending on the size of the gliding box used in computing the lacunarity value, the same pattern can return with very different values, as objects that are homogeneous at a small scale can be heterogeneous at a large scale (Plotnick et al., 1993). Myint and Lam (2005a, b) compared several hypothetical patterns; three of them are shown in Fig. 13.2. When a smaller gliding box of $3 \times 3$ is used, the small gap pattern (Fig. 13.2) results in low lacunarity (1.05), the big gap pattern yields the highest (1.40), and the random pattern yields a value in between (1.15). But when a bigger gliding box of $11 \times 11$ is used, the results are reverse, with the big gap pattern yielding the lowest lacunarity (1.02) and the small gap pattern the highest (1.10). Lacunarity value of the random pattern decreased slightly from 1.15 to 1.08. It is also observed that the range of difference between the two patterns is much smaller with bigger gliding box.

An algorithm for computing lacunarity using the gray-scale approach is described as follows (Voss, 1986; Myint and Lam, 2005a, b). Let $P(m, L)$ be the probability that there are $m$ intensity points within a cube size of $L$ centered at an arbitrary point in an image. Intensity points are points that fill the cube in each step. Hence, we have

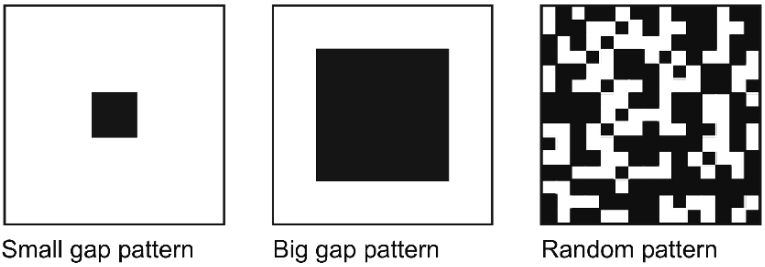


**Fig. 13.2** Three hypothetical binary patterns with different lacunarity values, see text for explanations. (Modified from Myint and Lam, 2005a.)

$$\sum_{m=1}^{N} P(m,L) = 1 \tag{13.3}$$

where $N$ is the number of possible points in the cube of $L$. Suppose that the total number of points in the image is $M$. If one overlays the image with cubes of side $L$, then the number of cubes with $m$ points inside the cube is *(M/m)P(m, L)*. Hence

$$M(L) = \sum_{m=1}^{N} mP(m,L) \tag{13.4}$$

and

$$M^2(L) = \sum_{m=1}^{N} m^2 P(m,L) \tag{13.5}$$

Lacunarity $\Lambda(L)$ can be computed from the same probability distribution *P(m, L)*, and is defined as:

$$\Lambda(L) = \frac{M^2(L) - (M(L))^2}{(M(L))^2} \tag{13.6}$$

Unlike fractals, lacunarity has no theoretical maximum or minimum. The performance of the index, especially its high scale dependency, will need to be further studied. However, a few studies have shown that adding a lacunarity layer in image classification has dramatically improved accuracy (Myint and Lam, 2005a, b), indicating a promising approach towards more accurate, automated land cover/land use mapping.

#### 13.2.3.4 The Wavelet Transform Method

Pioneered by Mallat (1989) and Daubechies (1990), the wavelet method has found numerous applications in a wide range of disciplines. The method has also recently been demonstrated as a promising approach to increasing accuracy in image classification and image retrieval using remote sensing imagery (Manjunath and Ma, 1996; Zhu and Yang, 1998; Bian, 2003; Myint et al., 2004).

In brief, wavelets are translated and dilated versions of a common mathematical function, called the mother wavelet. In the case of images, the translation refers to

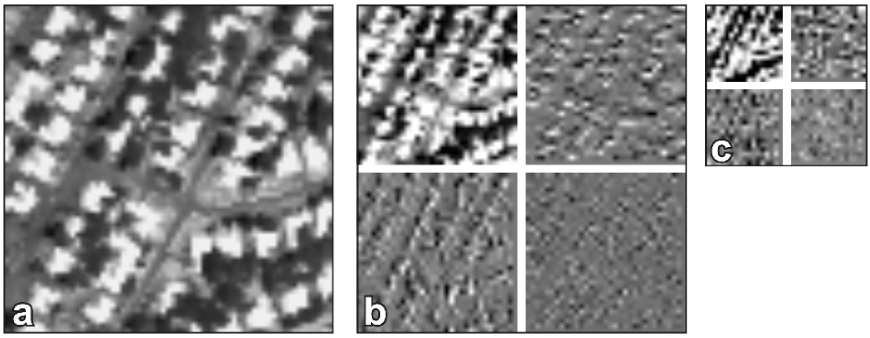


**Fig. 13.3** Multiresolution wavelet decomposition of a remote sensing image. (a) Original image, (b) level-1 decomposition: upper left is approximate sub-image, clockwise from upper left are horizontal, diagonal, and vertical detailed sub-images, (c) level-2 decomposition image (From Myint et al., 2004, reprint with permission from the American Society for Photogrammetry and Remote Sensing)

the geographic location, and the dilation relates to different scales. By adjusting the translation and dilation parameters, we can study the texture and scale locally. For the 2D discrete wavelet transform, which is used for remote sensing image analysis, the wavelet method will decompose an image into four sub-images: an approximate image (low frequency) and three detailed images (high frequency – horizontal, vertical, and diagonal). The approximate image can further be decomposed into another level, resulting in a multi-resolution wavelet analysis. Figure 13.3 shows an example of multiresolution wavelet decomposition. The coefficients of the four subimages are computed by Eqs. (13.7)–(13.10):

$$A(i,j) = \sum_k \sum_l h(k-2i)h(l-2j)f(k,l) \tag{13.7}$$

$$H(i,j) = \sum_k \sum_l h(k-2i)g(l-2j)f(k,l) \tag{13.8}$$

$$V(i,j) = \sum_k \sum_l g(k-2i)h(l-2j)f(k,l) \tag{13.9}$$

$$D(i,j) = \sum_k \sum_l g(k-2i)g(l-2j)f(k,l) \tag{13.10}$$

where $f$ is the original image, $A$ is the approximate image, $H$ is the horizontal detailed image, $V$ is the vertical detailed image, and $D$ is the diagonal detailed image. $h(k)$, $g(k)$ are the scaling filter and the wavelet filter, respectively, and $k$, $l$ are the number of rows and columns (Mallat, 1989; Daubechies, 1990).

After decomposition, indices can be computed for each sub-image at each level to represent the texture of the image. In addition to mean and standard deviation, Eqs. (13.11)–(13.14) show other commonly used measures (Myint et al., 2002), including log energy, Shannon index (SHAN), angular second moment (ASM), and entropy:

$$energy = \sum_{i=1}^{K} \sum_{j=1}^{K} \log(P(i,j)^2) \tag{13.11}$$

$$SHAN = -\sum_{i=1}^{K} \sum_{j=1}^{K} P(i,j) * \log(P(i,j)) \tag{13.12}$$

$$ASM = \sum_{i=1}^{K} \sum_{j=1}^{K} P(i,j)^2 \tag{13.13}$$

$$entropy = -\sum_{i=1}^{K} \sum_{j=1}^{K} Q(i,j) * \log|Q(i,j)|; Q(i,j) = \frac{|P(i,j)|^2}{\sqrt{\sum_{i,j} |P(i,j)|^2}} \tag{13.14}$$

where *P(i, j)* is the $(i, j)$th pixel wavelet coefficient value of a decomposed image at a particular level. These computed textural indices are then used to discriminate different types of land cover/land use.

### *13.2.4 Scale and Uncertainty in Textural Analysis*

Textural measures must be computed from a group of pixels or objects. Hence, texture is very scale-dependent. The size of the moving window combined with the resolution of the imagery plays a big part in determining what features are highlighted by these techniques. This scale and uncertainty issue has long been a central concern across a number of disciplines that involve geospatial/environmental data, textural analysis is not an exception. Scale variations are well known to constrain the detail with which information can be observed, represented, analyzed, and communicated (Lam et al., 2004).

It should be noted that the term "scale" has different meanings, and depending on the field of study, its meaning could be opposite. Lam and Quattrochi (1992) outlined four different meanings of scale (Cao and Lam, 1997). *Cartographic scale* refers to the degree of reduction in spatial dimensions that occurs when real-world measurements are represented in hard-copy maps or computer screens. *Operational scale* is an expression of the spatial or temporal dimensions over which a process operates, while *observational scale* refers to the dimensions within which a particular phenomenon or process is observed. *Measurement scale*, commonly called *resolution*, refers to the smallest observable unit, such as pixels in remote sensing imagery. In landscape ecology, observational scale is the *extent*, whereas measurement scale is referred to as *grain*. Radiometric scales also exist within digital imagery. Older Landsat Multispectral Scanner (MSS) images have a 6-bit grayscale depth, while IKONOS images have a 16-bit depth. One of the basic goals of scale-related research is to be able to move up and down spatial scales, within disciplines and across disciplines, so that the results concluded at one scale can be inferred to another

scale. Extrapolation of results across broad spatial scales remains the most difficult problem in environmental research (O'Neill et al., 1989; Turner et al., 1989; Lam and Quattrochi, 1992; Quattrochi and Goodchild, 1997; Tate and Atkinsons, 2001).

Scale affects change detection. The myriad spatial, spectral, radiometric, and temporal scales of remotely sensed imagery pose a real challenge to change detection, as techniques developed for imagery with a pixel resolution of 1 m (IKONOS imagery) may not be applicable to imagery with a pixel resolution of 1 km (AVHRR imagery). Since changes may occur at different scales, globally, regionally, or locally, and they may also occur rapidly or slowly, it is important to examine how change detection methods and indices perform at different spatial scales.

Scale-related uncertainty in modeling results has significant impacts on decision making, and basic research on decision making under uncertainty is necessary. Effective scale-related research requires interdisciplinary efforts of social, physical, and computer scientists. Scale and scale-related uncertainty is a difficult problem to tackle. Increasingly, it has been recognized that scale effects exist and can never be eliminated, therefore strategies must be developed to understand and mitigate the scale effects rather than to eliminate them. Two interrelated approaches were suggested to mitigate the scale effects (Lam et al., 2004). The first approach is to develop techniques to detect the scale ranges within which levels of observation are phenomena scale-dependent. Techniques such as geographic variance, variograms, correlograms, fractal analysis, and a number of textural methods have been proposed to detect the range of scales that yield the most information (Emerson et al., 1999). The second approach is to develop a multi-scale assessment module so that the same analysis can be conducted in multiple scales to compare the results and estimate the uncertainty. A thorough benchmark study is very much needed to examine how textural methods perform at different spatial scales and resolutions in land cover classification and change detection.

## 13.3 Land Cover Classification Using the Textural Approach: Examples

### *13.3.1 Characterizing Land Cover in the Tropics*

Read and Lam (2002) compared the performances of selected textural measures to characterize different land covers using two sets of unclassified Landsat-TM data (1986 and 1996/97) for a site in north-eastern Costa Rica. The purpose was to determine whether landscape complexity can be captured by these methods, and whether these methods can be used to reflect the degree of human disturbance. The hypothesis was that complexity in a natural landscape decreases with increasing intensity of human activities. The methods evaluated were: (1) fractal dimension using the isarithm method, (2) fractal dimension using the modified triangular prism method, (3) spatial autocorrelation using Moran's $I$, (4) Shannon's diversity index, (5) contagion, and (6) fractal dimension from perimeter/area. The first three methods

were available from ICAMS, and the last three were landscape metrics available from FRAGSTATS.

The results revealed that fractal dimension using the triangular prism method and Moran's *I* could serve as indices for characterizing spatial complexity of Landsat-TM data, whereas the landscape indices were not consistent. The fractal dimension decreased along a gradient of increasing human disturbance: forest–scrub–pasture–agriculture. This study is among the first to examine how spatial indices can be used to examine hypotheses related to land cover/land use and human disturbance in the tropics.

### *13.3.2 Improving Urban Land Cover Classification*

Emerson et al. (2005) examined the utility of local variance, fractal dimension, and Moran's *I* in improving urban land cover classification. Landsat ETM+ imagery of Atlanta, Georgia obtained in 1999 was examined. Using the routines in ICAMS, texture images were computed from the 15m panchromatic band using a $21 \times 21$ pixel moving window for every other row and column. This two-pixel increment between rows and columns produced a 30m resolution texture image. The real number local variance, Moran's *I*, and fractal dimension values (computed using the modified triangular prism method) were converted to 8-bit image, and they were added to the stack of multispectral bands for classification using a supervised maximum likelihood classification technique. Five land cover classes based on the USGS Anderson Level 1 classification scheme were used, including low intensity urban, high intensity urban, pasture/grassland, forest, and water.

Results show that classification accuracy improved with additional texture layer, with the fractal dimension band being the most effective. By adding the fractal dimension band to the multispectral bands, the overall percent correctly classified increased from 67.1% to 77.3%. Although not as effective as the fractal band, addition of local variance and Moran's *I* still yielded an improved accuracy of 72.4% and 69.4%, respectively. The results show great promise, but further research is needed to better utilize these indices.

### *13.3.3 Urban Feature Discrimination Using Wavelets*

Based on a high-resolution ATLAS (Advanced Thermal Land Application Sensor) image of Baton Rouge, Louisiana, USA, Myint et al. (2002, 2004) introduced the wavelet approach for urban land cover classification. The ATLAS image had a 2.5 m pixel resolution and was acquired with 15 channels (0.45–12.2 μm) from a NASA LearJet on May 7, 1999. Six urban land cover/land use classes with different texture appearances were selected, including agriculture, commercial, woodland, water body, single-family homes with less than 50% tree canopy (residential-1), and single-family homes with more than 50% tree canopy (residential-2). These land

cover classes were based on classification by Lo et al. (1997), which was designed for the purpose of urban planning, as information on surface vegetation and water availability are crucial for city officials and environmental agencies in developing better urban infrastructure. Based on previous studies, band 2 (0.52–0.60 μm), band 6 (0.76–0.90 μm), and band 12 (9.60–10.20 μm) were selected. In addition to these three bands, principal component analysis band 1 (PCA1) was also examined to see if a composite band could produce better accuracy.

Two segmented regions of each class were identified, and five training pixels were then randomly selected from each region, leading to a total of 10 samples for each class. Windows of $65 \times 65$, $33 \times 33$, and $17 \times 17$ pixels were selected using these 10 pixels as centers. Textural measures of these samples were computed and a linear discriminate analysis was applied to evaluate which measure is the most effective in discriminating the different land covers. Four different textural approaches were evaluated, including the wavelet transform, spatial autocorrelation, spatial co-occurrence matrix, and fractals. It was found from both studies that the wavelet approach was the most accurate among all approaches considered (Myint et al. 2002, 2004). When $65 \times 65$ samples were used, the wavelet approach yielded 100% accuracy. The overall accuracy, however, decreased with smaller window sizes, with an accuracy of 93% and 78%, respectively, for $33 \times 33$ and $17 \times 17$ samples. These studies demonstrated the great potential of using the texture approach. They also highlighted the importance of different scale parameters such as window size in affecting its performance. Future studies that systematically examine the effects of scale on the certainty, or rather uncertainty, of the results are needed.

### *13.3.4 Lacunarity-Based Urban Classification*

Myint and Lam (2005a, b) introduced the use of lacunarity in urban land cover/land use classification. As mentioned in Section 13.2.3, lacunarity measures the gappiness of a pattern; low lacunarity implies homogeneity, whereas high lacunarity suggests heterogeneity. An IKONOS image at 4 m spatial resolution with four channels acquired over Norman, Oklahoma, on March 20, 2000 was used. The selected land-use and land-cover classes in this study included single-family houses with less than 50% tree canopy (residential-1), single-family houses with more than 50% tree canopy (residential-2), commercial, woodland, agriculture, golf course, and water body. Lacunarity measures for band 4 (0.76–0.90 μm), band 3 (0.63–0.69 μm), and band 2 (0.52–0.60 μm) were computed for the entire image using the gray-scale method with a gliding cube of size 3 and a moving widow size of $29 \times 29$. The lacunarity-transformed bands were then stacked as additional bands for maximum likelihood classification.

The results show that adding three lacunarity transformed bands to the original three spectral bands (band 4, 3, 2) increased the overall classification accuracy from 55% to 92%, a drastic improvement. If only the three lacunarity transformed bands were used for classification, the overall accuracy still increased, but not substantially, to 68%. This study further confirmed the study by Emerson et al. (2005)

discussed above and demonstrated clearly that an integrated textural and spectral approach is needed for more accurate land cover/land use classification and mapping.

## 13.4 Land Cover/Land Use Change Analysis

Obviously, extending the mapping and modeling of land cover/land use at one time period to multiple time periods to analyze change adds lot more complexity and challenges. We outline in this section the inherent difficulties of change detection, summarize the existing methods into a framework, and then argue that the textural approach has potential for rapid change detection.

### *13.4.1 Change Detection Issues*

There are inherent difficulties involved in using time-series remote sensing data for land cover/land use change detection. Ideally, same type of images that have the same spectral, radiometric, spatial, and temporal resolutions should be used. However, this may not be possible especially for change studies that involve a longer time span. For example, Landsat-MSS with a pixel resolution of 80 m started in 1972, whereas Landsat-TM with a 30 m pixel resolution became available in 1982. Using digital imagery for change analysis before 1972 would be difficult. Often times, old aerial photographs before these dates are the only image sources to be used. The imminent danger of discontinuing global coverage due to sensor malfunction or budget constraints, such as Landsat-7 ETM+, will definitely hamper land cover/land use research and make long-term change analysis impossible.

When two very different types of images are involved, the only viable approach to change detection is to conduct detailed image classification of individual images and then overlay the two classified images to assess the changes. However, even with the same sensor, images taken in different dates may be affected by several factors, causing them to be different even if there is no real land cover change. Therefore, the following factors need to be considered for more accurate change detection:

1. The dates of the two images should be approximately the same to avoid seasonal difference in vegetation, soil moisture, sun-angle, and other response that are not real land cover change.
2. Even with the same date but in different years, individual atmospheric condition can obscure our ability to uncover real changes, such as cloud cover or rainfall. An image taken right after rainfall in a desert will look very different from an image of the same desert before rainfall. Atmospheric correction of each image may need to be applied before the analysis. For coastal landscape, tidal stage is a crucial factor in conducting change detection. Significant changes can be observed simply because the images were taken at different tidal stages (Jensen, 2005).

3. Pre-image processing steps may also contribute errors. Extra caution is needed to ensure no pixel mis-registration between the two images. A single pixel shift will shift the entire image and that could lead to substantial error in assessing change. Another point that has seldom been mentioned in the literature refers to the algorithm used to convert pixel values from analog to digital scale. Assuming an 8-bit scale (0–255) is used, some algorithms will convert the continuous signal using the image's minimum and maximum values as the limit, whereas others use the 99% or 95% interval. The result is that the same digital number in different images may have very different actual radiometric value, and the value is only true relative to the rest of the pixel values in its own image. Hence, change detection methods that involve direct pixel-by-pixel spectral comparison could be misleading, whereas change detection methods that are based on ratios among bands within its own image are more reliable. By the same token, it is expected that comparing the textural difference between two images, instead of pixel-by-pixel spectral comparison, would yield more accurate change analysis.

### *13.4.2 A Classification of Change Detection Methods*

New methods for change detection using remote sensing imagery have been continuously reported in the literature, and it is not the scope of this chapter to exhaust the list and provide evaluation of each approach. However, the following framework may be useful to classify the various change detection methods. Figure 13.4 shows how the various commonly used methods are placed in this framework.

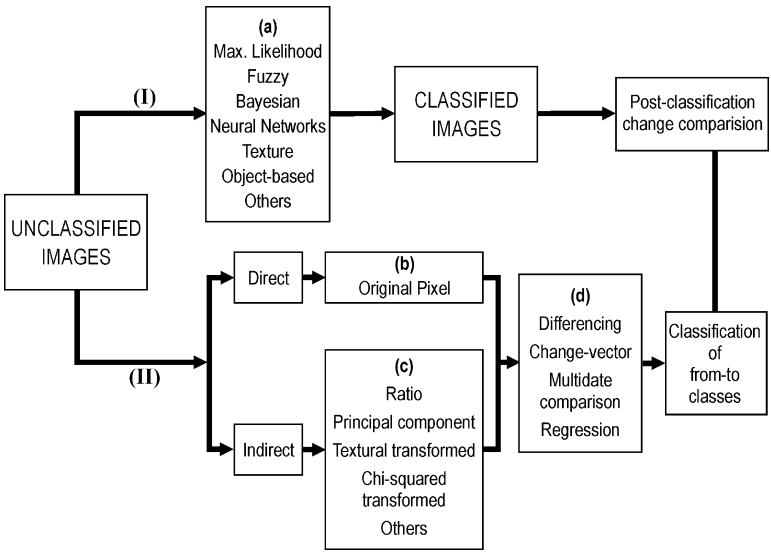


**Fig. 13.4** A framework for classifying change detection methods

Change detection methods can be differentiated into two main groups, depending on whether the method requires classification before or after the changes are detected. As shown in Fig. 13.4, the first group of change detection methods, which is also the most traditional approach to change detection, will first classify individual images of two dates using a statistical maximum likelihood classifier and then compare the classified images to provide an assessment of change. This traditional approach generally requires extensive human supervision for classifying the images. However, new image classification methods, other than the traditional maximum likelihood classifier, can be applied to increase accuracy and efficiency. These methods include, for example, fuzzy classification, artificial intelligence based classifier, Bayesian approach, and even the textural approach (Moller-Jensen, 1990; Gopal and Woodcock, 1996; Jensen, 2005; Gong, 2006). Recently, object-based image segmentation and classification has gained increasing attention, with new software such as eCognition (Definiens, 2004; Benz et al., 2004) and Feature Analyst (Visual Learning Systems, Inc.) made available to general users. These methods use both the spectral (or color) information and various spatial metrics to define homogenous areas (called objects). Despite its potential, this group of change detection methods is not germane to rapid change detection, as extensive human supervision is needed to pre-classify the images.

The second group of change detection methods does not require images to be pre-classified. Image differencing, change vector method, and multidate comparison methods (Fig. 13.4 – box d) can be applied directly to original pixel values or indirectly to modified values from the spectral bands (e.g., band ratios, principal components, chi-squared transformed, and texture transformed) (Fig. 13.4 – boxes b and c). The main advantage of this group of methods is that pre-classification is not necessary until significant changes are detected, hence avoiding the tedious classification process at the beginning. The problem remains to be that of determining the threshold value at which the difference between the two images is considered significant.

Continuous monitoring of land cover/land use and rapid identification of their changes is crucial to providing timely decision support and risk assessment especially during extreme events (e.g., hurricanes, earthquakes, forest fires, terrorist attacks, disease spread). There is a need to develop efficient and reliable change detection methods that can be automated, easy to use, and applicable to different land covers observed by different sensors at different scales, times, and places. Although it is difficult to achieve fully automated change detection, we expect that an integrated approach that incorporates both textural and spectral indices could alleviate some of the existing change detection problems for two reasons (which have also been elaborated in Section 13.2.2). First, the texture measures that have property 5 and 6 (e.g., fractals, lacunarity, wavelets, and spatial autocorrelation statistics) can be applied directly to pre-classified images without the need to go through the image classification process, thereby reducing the need for extensive human supervision upfront. Second, since the spatial/texture methods measure the spatial variations across the image instead of comparing brightness values on a pixel by pixel basis, they are more likely to reflect dominant changes rather than spurious changes that

occur due to noise, clouds, or illumination differences. However, whether a combination of these methods can be successfully applied to reliably characterize land covers and identify changes remains to be studied and is part of our ongoing research.

## 13.5 Change Detection Using the Textural Approach: An Example

In this section, we demonstrate the use of textural measures only (not including spectral information) for change detection in New Orleans before and after Hurricane Katrina. The utility of fractal dimension and spatial autocorrelation statistics in this capacity is compared. Hurricane Katrina hit New Orleans on August 29, 2005. Two Landsat-TM images, dated November 7, 2004 and September 7, 2005, were obtained from the US Geological Survey/National Wetlands Research Center at Louisiana State University and the LSU FEMA GIS Store project (http://www.cadgis.lsu.edu). Although not exactly the same anniversary dates, these two images are the best available so far for change detection. Both images have already been registered and geometrically rectified with a pixel resolution of 28.5 m prior to this study. For this study, we created a subset of $512 \times 512$ pixels from both images. Figure 13.5a and b display the subsets using band 4 (near-infrared band), which is the most effective band in discriminating water and non-water features. The subsets were mainly confined to the Orleans Parish, with a small part of the Lower Ninth Ward in St. Bernard Parish shown at the east edge of the image (east of the Industrial Canal breach). The post-Katrina image (Fig. 13.5b) clearly shows that most of New Orleans was flooded 9 days after Katrina, except in the natural levee area along the Mississippi River. The northwest corner of the image is Lake Pontchartrain, where significant storm surge has destroyed properties around the Lake. The three levee breaches at Industrial Canal, the 17th Street Canal, and the London Avenue Canal are also marked in Fig. 13.5b.

Both Landsat-TM images used in this example have previously been normalized to minimize sensor calibration offsets and differences in atmospheric effects. However, other factors may change the pixel values even though there are no real changes on the ground. A random check on the pixels at the northwest corner (Lake Pontchartrain) shows that a fair amount of difference in pixel values occurred in the same location between the two time periods (e.g., 32 vs 72 in pre- and post-Katrina image, respectively), even though no significant real change is expected at this location. This shows that change detection using the original spectral value pixel-by-pixel comparison approach alone could be problematic, especially regarding the determination of the threshold value to identify real changes.

Using ICAMS, we computed the local fractal dimension using the modified triangular prism algorithm and the local Moran's $I$ for each image. For the local fractal dimension method, the following parameters were used: moving window size of $17 \times 17$, step size of 5, stretch option, and arithmetic progression. For Morans' $I$,

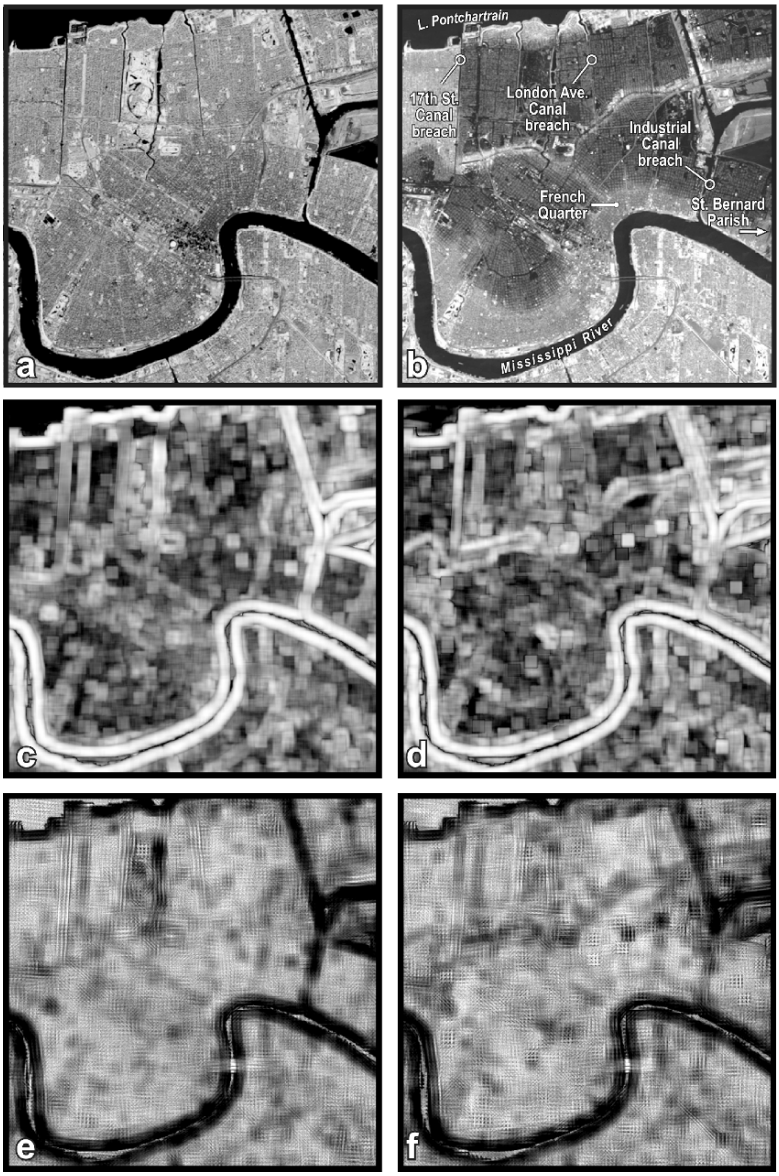


**Fig. 13.5** (a and b) Display of pre-Katrina (November 7, 2004) and post-Katrina (September 7, 2005) Landsat-TM images using band 4. (c) and (d) are Moran's *I* transformed pre- and post-images; (e) and (f) are fractal-transformed pre- and post-images

the only parameter needed to be input was the moving window size, which was also set to $17 \times 17$. The $17 \times 17$ window was chosen because a previous study on the impacts of Hurricane Hugo along the South Carolina's coast by Kulkarni (2004) found that this window size was the best in representing land cover features. Figure 13.5c–f

**Table 13.2** Summary statistics of band 4 for pre- and post-Katrina Landsat – TM images

| | Original | | | Fractal-transformed | | | Moran's *I*-transformed | | |
|---|---|---|---|---|---|---|---|---|---|
| | Pre | Post | Diff. | Pre | Post | Diff. | Pre | Post | Diff. |
| Min | 24.00 | 1.00 | −250.00 | 1.86 | 1.75 | −1.23 | −0.07 | −0.05 | −0.63 |
| Max | 255.00 | 255.00 | 96.00 | 4.11 | 4.13 | 1.15 | 0.97 | 0.97 | 0.63 |
| Mean | 161.50 | 45.02 | −116.49 | 2.77 | 2.74 | −0.03 | 0.61 | 0.66 | 0.05 |
| SD | 52.28 | 25.51 | 44.95 | 0.22 | 0.21 | 0.15 | 0.17 | 0.14 | 0.11 |
| CV | 0.32 | 0.57 | −0.38 | 0.08 | 0.08 | 5.00 | 0.28 | 0.21 | 2.20 |

SD – standard deviation; CV – coefficient of variation (= SD/mean); difference image = (post – pre)

show the Moran's *I*-transformed and the fractal-transformed images. Brighter pixels refer to higher values in fractal dimension or Moran's *I*. It should be stressed that since fractal dimension and Moran's *I* have an inverse relationship, features with low fractal dimension, such as the Mississippi River (darker pixels in the fractal-transformed images), will be shown as brighter pixels in the Moran's *I* transformed images.

The difference images were computed by subtracting the pre-Katrina image from the post-Katrina image, and the summary statistics of all images are listed in Table 13.2. In general, the post-image had lower spectral values than the pre-image, and the mean difference between the two images (band 4) was as high as −116.49. This is expected as most of the study area was flooded after Katrina, resulting in lower spectral reflectance value in the near-infrared band. The fractal-transformed summary statistics show that the mean spatial complexity, as represented by fractal dimension, slightly decreased from 2.77 to 2.74. Conversely, the mean Moran's *I* increased from 0.61 to 0.66, which also indicates that the overall spatial complexity decreased slightly for the post-image.

The fractal and Moran difference images were first mapped in a continuous mode (with a two-standard deviation stretch) using ICAMS. The fractal difference image (Fig. 13.6a) shows that increases in fractal dimension (positive changes), as represented by brighter pixels, occurred in areas close to the Industrial Canal (east side of the image) and the areas between the 17th Street Canal and London Avenue Canal (middle part of the image). Areas with decrease in fractal dimension (negative changes) are represented by darker pixels and they scattered over the image. With a $17 \times 17$ window size, the general features of the study area, such as the Mississippi River, can still be recognized. The Moran's *I* difference image (Fig. 13.6b) shows the same pattern; the darkest pixels represented the highest decrease in spatial autocorrelation, implying an increase in spatial complexity. It can be observed from the two difference images that the location of the darkest pixels in the Moran's *I* difference image generally coincided with the brightest pixels in the fractal different image, and vice versa.

The difference images can also be mapped using standard deviation unit as class intervals in ICAMS. One of the display options is to map the changes in three class intervals using two-standard deviations as class boundaries. The first interval, which contains pixels that have highest positive changes in spatial complexity

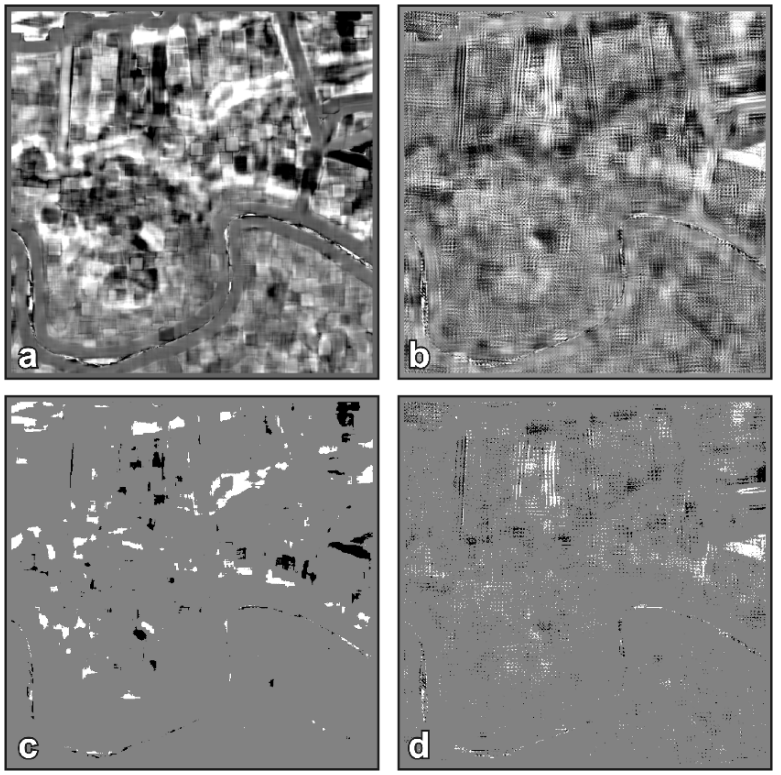


**Fig. 13.6** Display of the fractal-difference and Moran-difference images in a continuous mode (a) and (b) and three-class mode (c) and (d). In (c) and (d), the brightest pixels indicate the highest positive changes in spatial complexity (>2 standard deviations), the darkest pixels indicate highest negative changes (<−2 standard deviations), and the gray pixels are values in between. Both brightest and darkest pixels should be of interest, which may point to areas that are most "affected"

$(>2\,\mathrm{SD})$, is shaded as the brightest. The second class, which is in middle gray, is for pixels that have difference values falling between $\pm 2$ standard deviations. The third class, which has the darkest shade, is for pixels that have the greatest negative changes in spatial complexity $(<-2\mathrm{SD})$. Using this mapping method, both the brightest and the darkest pixels in the images (Fig. 13c and d) signal the greatest changes and hence attention is most warranted for these pixels and their surrounding pixels. This method should guide resources to the most "affected" areas, and in this case, greatest change in spatial complexity in both positive and negative directions.

Figure 13.6d, the fractal difference image, shows only a few concentrated spots belonging to the first and third classes (the brightest and darkest pixels), and they were generally located close to the three canal breach areas. The rest of the second-class pixels were scattered throughout the image. For the Moran difference image (Fig. 13.6c), because of its inverse relationship with fractal dimension (i.e., the higher the fractal dimension, the lower the Moran's $I$ value), one should expect that

the brightest spot in the fractal difference image would coincide with the darkest spot in the Moran's *I* difference image. A visual comparison between the two images (Fig. 13.6c and d) shows that this is generally true, with the Moran's *I* difference image portraying a wider area of brightest and darkest spots than the fractal difference image. Based on the Moran's *I* difference image (Fig. 13.6c), the greatest decrease in Moran's *I* values (greatest increase in spatial complexity – darkest pixels) were also found near the three canal breach areas. Areas that showed greatest increase in Moran's *I* values (greatest decrease in spatial complexity – brightest pixels) were scattered in the mid city and the area surrounding Lake Pontchartrain.

In summary, this example shows that the textural approach alone could be useful in pinpointing the areas that need the most attention. With additional information layers, these maps could serve as a useful guide to focus our efforts in detecting largest and meaningful changes in a rapid and reliable manner. It is expected that combining spectral and spatial layers, as well as combining different textural measures, will increase the accuracy of this approach. Other mapping methods could also be employed to further enhance the visualization of these changes.

## 13.6 Conclusions

Efficient methods for rapid monitoring of land cover/land use and their changes through remote sensing imagery are urgently needed to provide timely decision support and risk assessment especially during extreme events (e.g., terrorist attacks, hurricanes, forest fires, earth quakes, disease spread). Although there is a huge literature on land cover classification and change detection, we are still far from being able to automate these tasks via remote sensing and GIS. The high variability of ground conditions as manifested in individual as well as time-series imagery makes it very difficult to generalize and automate. The search for useful approaches and methods for rapid land cover identification and change detection remains a very challenging task.

This chapter introduced the use of textural and spatial metrics as a promising approach to automated land cover/land use classification and change detection. We identified in this chapter the major criteria for selecting textural measures and then illustrated through several examples from previous studies how textural metrics, in combination with the original spectral bands, have greatly improved the classification accuracy. For change detection analysis, we developed a framework for classifying the numerous change detection approaches. Then, using a recent example of evaluating the impacts of Hurricane Katrina on New Orleans land cover change, we illustrated the use of local fractal dimension and local Moran's *I* to detect the largest changes that might need further attention. More research is needed to determine the effectiveness of the various textural metrics with different types of remote sensing imagery, different scales and resolutions, different land cover features, and different environments. These issues are currently being examined in our ongoing research.

**Acknowledgements** John Barras, Geographer at the USGS/CR/BRD National Wetlands Research Center, Coastal Restoration Field Station, Louisiana State University, provided the Landsat-TM 2004 image data. Mary Lee Eggart assisted in preparing the figures. This research is supported in part by a NASA Intelligent Systems research grant (NCC-2-1246) and in part by a US National Science Foundation grant (BCS-0554937).

## References

Baskent EZ, Jordan GA (1955) Characterizing spatial structure of forest landscapes. Can. J. Forest Res. 25:1830–1849

Benz UC, Hofmann P, Willhauck G, Lingenfelder I, Heynen M (2004) Multi-resolution, object-oriented fuzzy analysis of remote sensing data for GIS-ready information. ISPRS J. Photogramm. Remote Sens. 58:239–258

Bian L (2003) Retrieving urban objects using a wavelet transform approach. Photogramm. Eng. Remote Sens. 69(2):133–141

Briggs JM, Nellis JM (1991) Seasonal variation of heterogeneity in the tallgrass prairie: A quantitative measure using remote sensing. Photogramm. Eng. Remote Sens. 57:407–411

Cao C, Lam NSN (1997) Understanding the scale and resolution effects in remote sensing and GIS. In: DA Quattrochi, MF Goodchild (eds), Scale in remote sensing and GIS. Lewis Publishers, Boca Raton, FL, pp 57–72

Carr JR (1999) Classification of digital image texture using variograms. In: PM Atkinson, NJ Tate (eds), Advances in remote sensing and GIS analysis. Wiley, London, pp 135–146

Carr JR, de Miranda FP (1998) The semivariogram in comparison to the co-occurrence matrix for classification of image texture. IEEE Trans. Geosci. Remote Sens. 36(6):1945–1952

Clarke KC (1986) Computation of the fractal dimension of topographic surfaces using the triangular prism surface area method. Comput. Geosci. 12(5):713–722

Clausi DA, Jobanputra R (2006) Preserving boundaries for image texture segmentation using grey level co-occurring probabilities. Pattern Recog. 39(2):234–245

Cliff AD, Ord JK (1973) Spatial autocorrelation. Methuen, New York

Coppin PR, Bauer ME (1966) Digital change detection in forest ecosystems with remote sensing imagery. Remote Sensing Reviews 13:207–234

Crews-Meyer KA (2002) Characterizing landscape dynamism using paneled-pattern metrics. Photogramm. Eng. Remote Sens. 68(10):1031–1040

Dale MRT (2000). Lacunarity analysis of spatial pattern: a comparison. Landscape Ecol. 15(5):467–478

Daubechies I (1990) The wavelet transform, time/frequency localization and signal analysis. IEEE Trans. Inf. Theory 36:961–1005

De Pietri DE (1995) The spatial configuration of vegetation as an indicator of landscape degradation due to livestock enterprises in Argentina. J. Appl. Ecol. 32:857–865

Definiens AG (2004) eCognition User Guide (accessed May 2006)

Dong P (2000) Test of a new lacunarity estimation method for image texture analysis. Int. J. Remote Sens. 21(17):3369–3373

Dunn CP, Sharpe DM, Guntenspergen GR, Stearns F, Yang Z (1991) Methods of analyzing temporal changes in landscape pattern. In: MG Turner, RH Gardner (eds), Quantitative methods in landscape ecology. The analysis and interpretation of landscape heterogeneity. Springer, New York

Emerson CW, Lam NSN, Quattrochi DA (1999) Multiscale fractal analysis of image texture and pattern. Photogramm. Eng. Remote Sens. 65(1):51–61

Emerson CW, Lam NSN, Quattrochi DA (2005) A comparison of local variance, fractal dimension, and Moran's I as aids to multispectral image classification. Int. J. Remote Sens. 26(8):1575–1588

Estreguil C, Lambin E (1996) Mapping forest disturbances in Papua New Guinea with AVHRR data. J. Biogeogr. 23:757–773

Falconer K (1988) Fractal geometry: mathematical foundations and applications. Wiley, New York

Frank TD (1984) The effect of change in vegetation cover and erosion patterns on albedo and texture of Landsat images in a semiarid environment. Ann. Assoc. Am. Geogr. 74:393–407

Franklin SE, Hall RJ, Moskal LM, Maudie AJ, Lavigne, MB (2000) Incorporating texture into classification of forest species composition form airborne multispectral images. Int. J. Remote Sens. 21(1):61–79

Gong P (2006) Information extraction. In: M Ridd, JD Hipple (eds), Remote sensing of human settlements. ASPRS, Bethesda, MD, pp 275–334

Gong P, Marceau DJ, Howarth PJ (1992) A comparison of spatial feature extraction algorithms for land use classification with SPOT HRV data. Remote Sens. Environ. 40:137–151

Goodchild MF (1980) Fractals and the accuracy of geographical measures. Mathematical Geology 12:85–98

Goodchild MF (1986) Spatial Autocorrelation. CATMOG (Concepts and Techniques in Modern Geography) No. 47. Geo Books, Norwich, England

Gopal S, Woodcock C (1996) Remote sensing of forest change using artificial neural networks. IEEE Trans. Geosci. Remote Sens. 34(2):398–404

Haralick RM (1979) Statistical and structural approaches to texture. Proc. IEEE 67(5):786–804

Haralick RM, Shanmugan K, Dinstein J (1973) Textural features for image classification. IEEE Trans. Syst. Man Cybern. 3(6):610–621

Jaggi S, Quattrochi D, Lam NSN (1993). Implementation and operation of three fractal measurement algorithms for analysis of remote sensing data. Comput. Geosci. 19(6):745–767

Jensen J, Cowen D, Althausen J, Narumalani S, Weatherbee O (1993) An evaluation of the Coast-Watch change detection protocol in South Carolina. Photogrammetric Engineering and Remote Sensing 59(6):1039–1046

Jensen J, Cowen D, Narumalani S, Halls J (1997) Principles of change detection using digital remote sensor data. In: JL Star, JE Estes, KC McGwire (eds), Integration of geographic information systems and remote sensing. Cambridge University Press, Cambridge, pp 37–54

Jensen J (2005) Introductory digital image processing: a remote sensing perspective, 3rd edn. Prentice-Hall, New Jersey

Jupp DLB, Walker J, Pendridge LK (1986) Interpretation of vegetation structure in Landsat MSS imagery: a case study in disturbed semi-arid eucalypt woodland. Part 2. model-based analysis. J. Environ. Manag. 23:35–57

Kulkarni A (2004) Evaluation of the Impacts of Hurricane Hugo on the Land Cover of Francis Marion National Forest, South Carolina Using Remote Sensing. M.S. thesis, Louisiana State University, Baton Rouge, Louisiana

Lam NSN (1990) Description and measurement of Landsat TM images using fractals. Photogramm. Eng. Remote Sens. 56(2):187–195

Lam NSN (2004) Fractals and scale in environmental assessment and monitoring. In: E Sheppard, R McMaster R (eds), Scale and Geographic Inquiry: Nature, Society, and Method. Blackwell, Oxford, pp 23–40

Lam NSN, Quattrochi DA (1992) On the issues of scale, resolution, and fractal analysis in the mapping sciences. Prof. Geogr. 44(1):89–99

Lam NSN, De Cola L (eds) (1993) Fractals in geography. Prentice-Hall, Englewood Cliffs, NJ, 308p

Lam NSN, Quattrochi DA, Qiu HL, Zhao W (1998) Environmental assessment and monitoring with image characterization and modeling system using multiscale remote sensing data. Appl. Geogr. Stud. 2(2):77–93

Lam NSN, Qiu HL, Quattrochi DA, Emerson CW (2002) An evaluation of fractal methods for measuring image complexity. Cartogr. Geogr. Inform. Sci. 29:25–35

Lam NSN, Catts C, Quattrochi DA, Brown D, McMaster R (2004) Scale. In: R McMaster, L Usery (eds), A Research Agenda for Geographic Information Science. CRC Press, Bacon Raton, FL, Chapter 4, pp 93–128

Lambin EF (1996) Change detection at multiple temporal scales: seasonal and annual variations in landscape variables. Photogramm. Eng. Remote Sens. 62:931–938

Lambin EF, Strahler AH (1994) Indicators of land-cover change for change-vector analysis in multitemporal space at coarse spatial scales. Int. J. Remote Sens. 15:2099–2119

Lo CP, Quattrochi DA, Luvall JC (1997) Application of high-resolution thermal infrared remote sensing and GIS to assess the urban heat island effect. International Journal of Remote Sensing 18(2):287–304

Lu D, Mausel P, Brondizio E, Moran E (2005) Land-cover binary change detection methods for use in the moist tropical region of the Amazon: a comparative study. Int. J. Remote Sens. 26(1):101–114

Lunetta R, Elvidge C (1998) Remote sensing change detection: environmental monitoring methods and applications. Sleeping Bear Press, Ann Arbor, MI

Mallat SG (1989) A theory for multi-resolution signal decomposition: the wavelet representation. IEEE Trans. Pattern Anal. Machine Intell. 11:674–693

Mandelbrot B (1982) The fractal geometry of nature. Freeman, New York

Manjunath BS, Ma WY (1996) Texture features for browsing and retrieval of image data. IEEE Trans. Pattern Anal. Machine Intell. 18(8):837–842

Mark DM, Aronson PB (1984) Scale-dependent fractal dimensions of topographic surfaces: an empirical investigation, with applications in geomorphology and computer mapping. Math. Geol. 11:671–684

Mas JF (1999) Monitoring land-cover changes: a comparison of change detection techniques. Int. J. Remote Sens. 20:139–152

McGarigal K (2002) Landscape pattern metrics. In AH El-Shaarawi, WW Piegorsch (eds), Encyclopedia of environmentrics, vol 2. Wiley, Sussex, England, pp 1135–1142

McGarigal K, Mark BJ (1995) FRAGSTATS: spatial pattern analysis program for quantifying landscape structure. USDA Forest Service General Technical Report PNW-351, Portland, Oregon

Mallat, S (1989) A theory of multi-resolution signal decomposition: the wavelet representation. IEEE Trans. Pattern Anal. Machine Intel. 11:674–693

Moller-Jensen L (1990) Knowledge-based classification of an urban area using texture and context information in Landsat-TM imagery. Photogramm. Eng. Remote Sens. 56(6):899–904

Muneeswaran K, Ganesan L, Arumugam S, Sounda KR (2005) Texture classification with combined rotation and scale invariant wavelet features. Pattern Recogn. 38(10):1495–1506

Myint S, Lam NSN (2005a) A study of lacunarity based texture analysis approaches to improve urban image classification. Comput. Environ. Urban Syst. 29:501–523

Myint S, Lam NSN (2005b) Examining lacunarity approaches in comparison with fractal and spatial autocorrelation techniques for urban mapping. Photogramm. Eng. Remote Sens. 71(8):927–937

Myint S, Lam NSN, Tyler J (2002) An evaluation of four different wavelet decomposition procedures for spatial feature discrimination in urban areas. Trans. GIS 6(4):403–429

Myint S, Lam NSN, Tyler J (2004) Wavelets for urban spatial feature discrimination: Comparisons with fractals, spatial autocorrelation, and spatial co-occurrence approaches. Photogramm. Eng. Remote Sens. 70(8):803–812

Nackaerts K, Vaesen K, Muys B, Coppin P (2005) Comparative performance of a modified change vector analysis in forest change detection. Int. J. Remote Sens. 26(5):839–852

O'Neill RV, Johnson AR, King AW (1989). A hierarchical framework for the analysis of scale. Landscape Ecol. 7(1):55–61

O'Neill RV, Krummel JR, Gardner RH, Sugihara G, Jackson B, DeAngelis DL, Milne BT, Turner MG, et al. (1998) Indices of landscape pattern. Landscape Ecol. 1:153–162

Openshaw S (1989) Automating the search for cancer clusters. Prof. Statistician 8:7–8

Pickup G, Foran BD (1987) The use of spectral and spatial variability to monitor cover change on inert landscapes. Remote Sens. Environ. 23:351–363

Plotnick RE, Gardner RH, O'Neill RV (1993) Lacunarity indices as measures of landscape texture. Landscape Ecol. 8:201–211

Quattrochi DA, Goodchild MF (1997) Scale in remote sensing and GIS. CRC/Lewis Publishers, Boca Raton, FL

Quattrochi DA, Lam NSN, Qiu HL, Zhao W (1997) Image characterization and modeling system (ICAMS): a geographic information system for the characterization and modeling of multiscale remote sensing data. In: D Quattrochi, M Goodchild (eds), Scaling in remote sensing and GIS. CRC/Lewis Publishers, Boca Raton, FL, pp 295–307

Read JM, Lam NSN (2002) Spatial methods for characterizing land-cover changes for the tropics. Int. J. Remote Sens. 23(12):2457–2474

Smits PC, Annoni A (2000) Towards specification-driven change detection. IEEE Trans. Geosci. Remote Sens. 38:1484–1488

Tate N, Atkinsons P (eds) (2001) Modelling scale in geographical information science. Wiley, New York

Turner MG, Dale VH, Gardner RH (1989) Predicting across scales: theory development and testing. Landscape Ecol. 3(3/4):245–252

Voss R (1986) Random fractals: characterization and measurement. In: R Pynn, A Skjeltorp (eds), Scaling phenomena in disordered systems. Plenum, New York

Woodcock CE, Strahler (1987) The factor of scale in remote sensing. Remote Sens. Environ. 21:311–332

Yuan D, Elvidge C, Lunetta R (1998) Survey of multispectral methods for land cover change analysis. In: R Lunetta, D Elvidge (eds), Remote sensing change detection. Sleeping Bear Press, Ann Arbor, MI

Zhu C, Yang X (1998) Study of remote sensing image texture analysis and classification using wavelet. Int. J. Remote Sens. 19(16):3197–3203